International Journal of Biochemistry and Cell Biology 121 (2020) 105700

Contents lists available at ScienceDirect

International Journal of Biochemistry and Cell Biology

journal homepage: www.elsevier.com/locate/biocel

Mechanism of miR-222 and miR-126 regulation and its role in asbestos-induced malignancy

Simona Gaetani[a], Federica Monaco[a], Federica Alessandrini[b], Adriano Tagliabracci[b], Armando Sabbatini[c], Massimo Bracci[a], Matteo Valentino[a], Jiri Neuzil[d,e], Monica Amati[a], Lory Santarelli[a,*], Marco Tomasetti[a,*]

[a] Department of Clinical and Molecular Sciences, Section of Experimental and Occupational Medicine, Polytechnic University of Marche, Via Tronto 10/A, 60020, Ancona, Italy
[b] Department of Biomedical Sciences and Public Health, Section of Legal Medicine, Polytechnic University of Marche, Via Tronto 10/A, 60020, Ancona, Italy
[c] Division of Thoracic Surgery, United Hospitals, Ancona, 60126, Italy
[d] Mitochondria, Apoptosis and Cancer Research Group, School of Medical Science, Griffith University, Southport, 4222, Qld, Australia
[e] Molecular Therapy Group, Institute of Biotechnology, Czech Academy of Sciences, Prague-West, 252 50, Czech Republic

ARTICLE INFO

Keywords:
miR-222
miR-126
Asbestos exposure
EGFR pathway
Epigenetic alterations

ABSTRACT

MiR-222 and miR-126 are associated with asbestos exposure and the ensuing malignancy, but the mechanism(s) of their regulation remain unclear. We evaluated the mechanism by which asbestos regulates miR-222 and miR-126 expression in the context of cancer etiology. An 'in vitro' model of carcinogen-induced cell transformation was used based on exposing bronchial epithelium BEAS-2B cells to three different carcinogens including asbestos. Involvement of the EGFR pathway and the role of epigenetics have been investigated in carcinogen-transformed cells and in malignant mesothelioma, a neoplastic disease associated with asbestos exposure. Increased expression of miR-222 and miR-126 were found in asbestos-transformed cells, but not in cells exposed to arsenic and chrome. Asbestos-mediated activation of the EGFR pathway and macrophages-induced inflammation resulted in miR-222 upregulation, which was reversed by EGFR inhibition. Conversely, asbestos-induced miR-126 expression was affected neither by EGFR modulation nor inflammation. Rather than methylation of the miR-126 host gene *EGFL7,* epigenetic mechanism involving DNMT1- and PARP1-mediated chromatin remodeling was found to upregulate of miR-126 in asbestos-exposed cells, while miR-126 was downregulated in malignant cells. Analysis of MM tissue supported the role of PARP1 in miR-126 regulation. Therefore, activation of the EGFR pathway and the PARP1-mediated epigenetic regulation both play a role in asbestos-induced miRNA expression, associated with in asbestos-induced carcinogenesis and tumor progression.

1. Introduction

MicroRNAs (miRNAs, miRs) play a role in many molecular pathways, and their expression is modulated by different stimuli. Among them, the environmental exposure to metals and air pollution can cause miRNA alterations via increasing oxidative stress and/or triggering inflammatory responses (Ferrante and Conto, 2017). Recently, miR-222 and miR-126 were identified to be associated with chemical and asbestos exposure (Vriens et al., 2016; Deng et al., 2019; Ruíz-Vera et al., 2019; Santarelli et al., 2019). MiR-222 and miR-126 are angiogenesis-related miRNAs involved in regulation of the vasculature. Both miRNAs have been extensively studied in human malignancies. MiR-126 was found mainly downregulated in cancer tissues, while miR-222 was increased in several malignancies, and both miRNAs contribute to poor prognosis (Matsuzaki et al., 2015; Wei et al., 2016; Song et al., 2017). Overexpression of miR-222 can contribute to estrogen-independent growth and resistance in breast cancer (Rao et al., 2011). On the other hand, downregulation of miR-126 correlates with the pathological characteristics of malignant mesothelioma (MM), such as the tumor size, lymph node metastasis, and advanced TNM stage (Ebrahimi et al., 2014).

Regulation of miRNA expression includes various mechanisms, such as epigenetic changes (methylation), or regulation of transcription factors that control expression of miRNA-coding genes. DNA methylation-induced silencing of miR-126 and its host gene EGFL7 was found in breast cancer (Zhang et al., 2013), lung cancer (Liu et al., 2018; Du

* Corresponding authors.
E-mail addresses: l.santarelli@univpm.it (L. Santarelli), m.tomasetti@staff.univpm.it (M. Tomasetti).

https://doi.org/10.1016/j.biocel.2020.105700
Received 26 July 2019; Received in revised form 22 January 2020; Accepted 27 January 2020

et al., 2015), esophageal squamous cell carcinoma (Liu et al., 2015), glioma (Cui et al., 2016) and malignant mesothelioma (Andersen et al., 2015). Our previous study showed that miR-222 and miR-126 are associated with asbestos-induced thoracic malignancies, but their role and mechanism of action in asbestos-induced pathogenesis are not fully elucidated (Santarelli et al., 2019).

In the present study, an 'in vitro' asbestos-induced carcinogenesis model was used to evaluate the mechanism by which miR-222 and miR-126 are modulated in response to asbestos exposure.

2. Materials and methods

2.1. Ethic statement

This study was performed according to the Helsinki Declaration, and sample processing was approved by the Ethical Committee of the University Hospital of Marche, N. 51/DG 05/02/2009.

2.2. Patients and tissue samples

Patients with MM were diagnosed at the Clinic of Pneumology and Thoracic Surgery of the Ancona University Hospital (Italy) in the period 2011–2017. Diagnostic biopsies were sampled from 6 MM male patients, with the median age of 68.7 ± 6.0 years, with the following histotypes: 5 epithelioid MM (EMM), 1 sarcomatoid MM (SMM), prior to neoadjuvant chemotherapy or cytoreductive surgery.

2.3. Cell culture and treatments

Immortalized human bronchial epithelial cells (BEAS-2B), human monocyte U937 cells, fibroblasts (IMR-90), non-malignant mesothelial cells (Met-5A), and malignant mesothelioma cells (H28) were obtained from ATCC. BEAS-2B and IMR-90 cells were grown in DMEM, while U937, Met-5A and H28 cells were cultured in the RPMI medium (Invitrogen), both supplemented with 10 % FBS, 1 % penicillin and 1 % streptomycin. Human umbilical vein endothelial cells (HUVECs) obtained from GIBCO (Life Technologies) were grown in Medium 200 with the large vessel endothelial supplement (LVES; Life Technologies). The cells were cultured in a humidified incubator at 37 °C and 5 % of CO_2, and maintained in culture for up to six passages within 1 month after placing them into culture; the cells were evaluated for mycoplasma contamination using the PCR Mycoplasma Test.

Crocidolite asbestos fibres were suspended in PBS and diluted in complete culture medium to the final concentration of 5 μg/cm^2. Sodium arsenite ($NaAsO_2$; Sigma) and potassium chromate ($K_2Cr_2O_7$; Sigma) in PBS were diluted in complete culture medium to the final concentration of 1 μM and 0.5 μM, respectively. The EGFR inhibitor AG1478 (Sigma) was added to the culture medium at 10 μM for 24 h from a 10 mM stock solution in DMSO. The DNMT inhibitor 5-aza-2'-deoxycytidine (5-aza-dC, Sigma), the PARP1 inhibitor 3-aminobenzamide (3-ABA) were added to culture medium at 5 μm for 96 h and 0.5 mM for 24 h, respectively.

2.4. PARP1 silencing

PARP1 was stably silenced in Met-5A and H28 cells by transfection with the PARP1 shRNA pRS plasmid (1 μg) carrying the PARP1 targeting sequence of TAC CAT CCA GGC TGC TTT GTC AAG AAC AG using the TransIT-LT1 transfection reagent (Mirus). Negative control cells were transfected with 1 μg of empty pRS plasmid (OriGene). Selection was performed with puromycin (1 μg/ml) for 48 h post-transfection. Selected clones were isolated, expanded, and maintained in medium with puromycin (1 μg/ml). PARP1 levels were analyzed by quantitative RT-PCR.

2.5. Selection of transformed cells

BEAS-2B cells (10^4) were grown in a 6-well plate and sodium arsenite (1 μM), crocidolite asbestos fibres (5 μg/cm^2), and potassium chromate (0.5 μM) were added to the media from freshly prepared aqueous filter-sterilized solutions. The cells were cultured in the presence of carcinogens and split every third day. After 4 weeks of incubation, the carcinogen-exposed cells were seeded in low-melting point agar (0.7 %) in 24-well plates, overlaid with 0.35 % low-melting point agar, and cultured at 37 °C in 5 % CO_2 for 3 months. Every 7 days, 0.5 ml of fresh complete medium was replaced in each well. The colonies greater than 0.1 mm in diameter were collected and grown in complete DMEM medium. No colony formation was found in control BEAS-2B cells that were not exposed to the carcinogens.

2.6. Co-culture model

Fibroblast IMR-90 cells (10^5) were seeded on a 3-μm trans-well insert (Costar 3452; Corning) in an inverted position. After incubation (6 h), inserts were flipped over and placed into a six-well trans-well plate, where HUVECs (3×10^5) were placed on the other side of the insert and cultured for 24 h. This IMR-90-HUVEC pre-coated trans-well inserts were then placed into another six-well trans-well plate, where asbestos-transformed BEAS-2B cells (2×10^5) had been plated. After 2 days of incubation, the cells were collected and the level of miRNAs and gene expression evaluated.

2.7. Macrophage-induced cytokine production

Human leukemic monocyte U937 cells were used as an *in vitro* model of inflammation induction. U937 cells were differentiated into macrophage-like cells (MLCs) by treatment with 50 nM phorbol myristate acetate (PMA; Sigma) for 24 h. Differentiated MLCs were co-cultured with BEAS-2B or carcinogen-transformed BEAS-2B in a six-well trans-well plate, and then activated by lipopolysaccharide (LPS, 1 μg/ml; Sigma) to stimulate production of pro-inflammatory cytokines (Nakamura et al., 2012). After 72-h incubation, parental and transformed BEAS-2B cells were collected and miRNA expression evaluated.

2.8. Evaluation of glucose uptake and glucose, lactate, and intracellular ATP levels

For glucose uptake, parental and transformed BEAS-2B cells (3×10^4 cells per well) grown at low glucose (1 g/l) DMEM were treated with 2-nitrobenzodeoxyglucose (2-NBDG, 50 μM) for 30 min. Fluorescence intensity was evaluated at 550/590 nm using a plate reader (Infinite F200 PRO, Tecan). Parental and carcinogen-transformed BEAS-2B cells were treated with rotenone (20 μM, 5 h) to inhibit OXPHOS and with 2-deoxyglucose (5 mM, 5 h) to inhibit glycolysis, and the levels of glucose, lactate and intracellular ATP were evaluated using commercial kits (Abcam) according to the manufacturer's protocol. The results were normalized to the total protein content.

2.9. ROS detection

Intracellular and mitochondrial reactive oxygen species (ROS and mtROS) were evaluated using fluorescent dyes 2′7′-dichlorofluorescein diacetate (DCFDA) and dihydroethidium (DHE), respectively. Parental and transformed BEAS-2B cells (2×10^5) were seeded in 6-well plates and supplemented with 20 μM DCFDA or DHE per well. After 30 min of incubation the cells were washed, re-suspended in PBS, and analyzed by flow cytometry (FACS Calibur, Becton Dickinson). The level of ROS was expressed as mean fluorescence intensity (MIF).

2.10. Quantitative RT-PCR

Total RNA from cultured cells and tissue samples was obtained using the RNeasy Mini Kit (Qiagen). MiRNAs first-strand cDNA was synthetized using the TaqMan miRNA Assay (Applied Biosystems, Life Technologies) according to the manufacturer's instructions. The qRT-PCR reactions were carried out using the TaqMan® Fast Advanced Master gene expression kit (Applied Biosystems, Life Technologies) at the following conditions: 50 °C for 2 min, 95 °C for 20 s, 40 cycles of 95 °C for 1 s and 60 °C for 20 s, 4 °C. U6 was used for normalization. The EGFL7, DNMT1 and PARP1 gene expression was evaluated using high capacity cDNA reverse transcription kit (Applied Biosystems) and qRT-PCR was performed using SYBR Green Master Mix (Applied Biosystems) with GAPDH as the housekeeping gene. The qRT-PCR assays were performed using Realplex Mastercycler epgradient S (Eppendorf), results were expressed as relative level ($2^{-\Delta CT}$) and fold change ($2^{-\Delta\Delta CT}$).

2.11. Detection of DNA-methylation

Genomic DNA was extracted from fresh tissues and cells using the QIAamp DNA Mini Kit (Qiagen). Bisulfite treatment was performed using the EZ DNA Methylation™ Kit (Zymo Research, Euroclone) according to the manufacturer's instructions. The methylation status of the host gene *EGFL7* T2 promoter was analyzed using the following specific primer pairs: forward, 5′-TTG GGT TTT GTT ATG TGG TTT TAG-3′; reverse, 5′-AAC CCT TTA CTA ACT TTC AAA CCC-3′. PCR products were purified with Exonuclease I (EXO I) and Calf Intestinal Alkaline Phosphatase (CIP) according to the manufacturer's instructions. The purified PCR products were sequenced using the reverse primer (5′-AAC CCT TTA CTA ACT TTC AAA CCC-3′) and the BigDye™ Terminator v1.1 Cycle Sequencing Kit (ThermoFischer Scientific) and then purified with the BigDye XTerminator™ Purification kit (ThermoFischer Scientific) according to the manufacturer's instructions. Capillary electrophoresis was performed on the 3500 Genetic Analyzer (ThermoFischer Scientific) and data were analyzed with the Sequence Analysis software v6 (ThermoFischer Scientific).

2.12. Western immunoblotting

Cells were lysed in the RIPA buffer supplemented with Na_3VO_4 and protease inhibitors. Proteins were separated using 4–12 % blot-SDS precast gels (Life Technologies) and transferred onto nitrocellulose membranes (Protran). Membranes were incubated with antibodies against EGFR, phospho-EGFR, IRS1 (all Bethyl), AKT, phospho-AKT, ERK1/2, phospho-ERK1/2, p38MAPK, phospo-p38 MAPK (Cell Signaling). β-actin was used as loading control. After incubation with the HRP-conjugated secondary IgG (Sigma), the blots were processed with the ECL detection system (Pierce Biotechnology). Band intensities were visualized and quantified with ChemiDoc using the Quantity One software (BioRad Laboratories).

2.13. Statistical analysis

Results are expressed as mean ± SD. Two-tailed Student's *t*-test was used to compare two groups. For comparison of more than two groups, one-way ANOVA with Tukey post-hoc analysis was performed. Correlations were performed according to the Spearman's test. Differences with $p < 0.05$ were considered statistically significant. All data generated in this study were analyzed using the SPSS software).

3. Results

3.1. MiR-222 and miR-126 are upregulated in asbestos-transformed epithelial cells

Three different carcinogens involved in lung cancer onset, arsenic (As), crocidolite (Asb), and hexavalent chrome (Cr) were used to induce cell transformation of BEAS-2B cells. After one month of exposure to the carcinogens, the surviving cells were collected. A single-cell suspension of the carcinogen-exposed cell population was seeded into soft agar in order to assess their ability to proliferate in an anchorage-independent manner, a key step in the transition of a normal cell into a malignant cell. Isolated colonies that arose from individual cells were removed from the agar and grown as a monolayer for a number of cell divisions in the absence of carcinogens. As showed in Supplementary Fig. 1, the cells with acquired transformed phenotype ('initiated' cells) grew in agar suspension cultures, forming colonies. Of the three types of transformed cells, chrome-transformed cells (BEAS-2B^{Cr}) showed the highest proliferation rate, while the highest rate of ROS formation (intracellular and mitochondrial) was observed in arsenic-transformed cells (BEAS-2B^{As}). Carcinogen-transformed cells showed increased mitochondrial potential associated with increased mitochondrial redox activity (MRA), which was significantly higher in asbestos-transformed cells (BEAS-2B^{Asb}). Metabolic changes were observed in all transformed cells showing increased glucose uptake associated with low intracellular glucose (high rate glucose consumption) and increased lactate production without affecting ATP levels. Inhibition of OXPHOS by rotenone resulted in further increase of lactate levels, which was inhibited by 2DG, suggesting a shift to glycolysis (Supplementary Fig. 2).

Among the used carcinogens, asbestos induced miR-222 and miR-126 expression in a time-dependent manner, peaking on day 14 of the incubation (Fig. 1A, B). Both miRNAs were highly expressed in BEAS-2B^{Asb} cells and their expression further increased in a cancer stroma model, where the cells were co-cultured with fibroblasts and endothelial cells in order to check the effect of the microenvironment (Fig. 1C).

3.2. Asbestos exposure induces miR-222 expression by activation of the EGFR pathway

It has been suggested that aggregation of EGFR in response to exposure to long asbestos fibers initiates cell signaling cascades resulting in carcinogenesis (Pache et al., 1998; Carbonari et al., 2011). EGFR was found highly expressed in the asbestos-transformed cells, causing activation of the downstream AKT and p38 MAPK signaling (Fig. 2A, B).

To investigate the involvement of the EGFR pathway in asbestos-induced miRNA expression, miR-222 and miR-126 level was evaluated in the transformed cells in the absence and presence on the EGFR inhibitor AG1478. Inhibition of the EGFR pathway significantly reduced asbestos-induced miR-222 expression, while increasing miR-126 level in BEAS-2B^{Asb} cells (Fig. 2C). Inflammatory cytokines were found to induce miR-222 expression, and exposure to asbestos further increased its expression by a mechanism involving EGFR activation. Conversely, asbestos-induced miR-126 expression was not affected by inflammation and was independent of EGFR (Fig. 2D).

3.3. Epigenetic regulation of asbestos-induced miR-126 expression

To uncover the mechanism by which miR-126 is upregulated in asbestos-transformed BEAS-2B cells, we studied methylation-associated regulation of the miR-126 host gene *EGFL7*. As shown in Fig. 3A, no changes in the DNA methylation status were observed in BEAS-2B^{Asb} cells compared to controls. To further explore the mechanism of miR-126 upregulation, enzymes related to epigenetic events such as DNMT1 and PARP1 were studied in asbestos-transformed cells. Fig. 3B shows that high expression of miR-126 and its host gene *EGFL7* found in BEAS-2B^{Asb} cells is associated with increased expression of DNMT1 and reduced expression of PARP1 in monoculture of the cells, while these parameters are enhanced in BEAS-2B^{Asb} cells co-cultured within the stroma model. Immunocytochemical analysis showing increased DNMT1 level and reduced PARP1 expression in BEAS-2B^{Asb} cells further supports these results (Fig. 3C, D). Next, the role of DNMT1 and

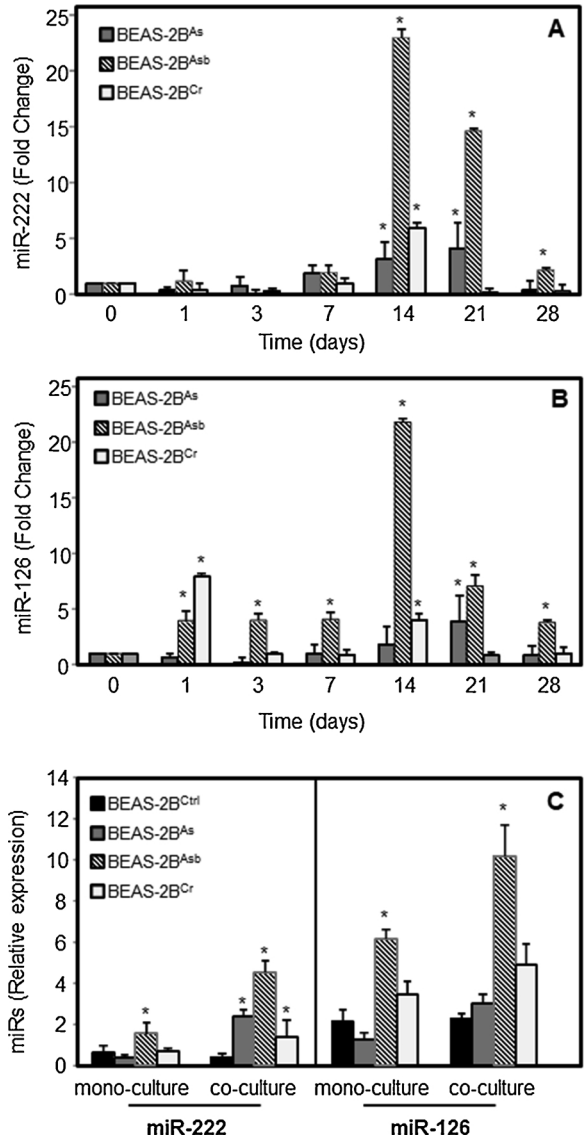

Fig. 1. Kinetics of miR-222 and miR-126 expression after carcinogen exposure. BEAS-2B cells were exposed to sodium arsenate (As, 1μM), crocidolite fibers (Asb, 5 μg/cm^2) and potassium dichromate (Cr, 0.5μM), and the level of miR-222 (A) and miR-126 (B) expressed as fold change respect to control cells (BEAS-2B^{Ctrl}) were assessed at different time points. C) The level of miR-222 and miR-126 in control and carcinogen-transformed BEAS-2B cells mono-cultured or co-cultured in a stroma model with fibroblasts (IMR-90) and endothelial cells (HUVEC). The symbol '*' indicates significant differences compared to non-exposed control cells, with $p < 0.05$.

PARP1 in the modulation of asbestos-induced miRNA expression was examined in the BEAS-2B cells and their asbestos-transformed counterpart by inhibiting DNMT1 with 5-aza-dC, PARP1 with 3-ABA, or both DNMT1 and PARP1. Inhibition of DNMT1 or PARP1 activity markedly reduced expression of miR-126 in BEAS-2B^{Asb} cells, supporting their involvement in asbestos-induced miRNA expression (Fig. 3E).

3.4. DNMT1 and PARP1 as regulators of miR-126 and miR-222 expression in malignant mesothelioma

MM is a malignancy originating from the mesothelium of the pleural and peritoneal cavities associated with asbestos exposure. One month of continuous asbestos exposure of non-malignant mesothelial cells (Met-5A) increased the expression of miR-222 via a mechanism that involves EGFR signaling, while no change was observed for miR-126 (Fig. 4A). Indeed, asbestos exposure induced the expression of DNMT1 and reduced the level of PARP1 (Fig. 4B). To evaluate their role in miRNA regulation, Met-5A and H28 cells were treated with 5-aza-dC, or silenced for PARP1, or treated with both 5-aza-dC and PARP1 siRNA. Low expression of miR-126 was found in the malignant H28 relative to the non-malignant Met-5A (Fig. 4C). Treatment with 5-aza-dC restored the expression of miR-126 and its host gene *EGFL7* in the cells, suggesting involvement of methylation (Fig. 4C, F). The increased miR-126 level was associated with increased DNMT1 and reduced PARP1 expression. Knocking down PARP1 induced DNMT1 expression and reduced miR-126 expression, which was further reduced when both DNMT1 and PARP1 were inhibited (Fig. 4F).

Conversely, DNMT1 inhibition reduced miR-126 level in Met-5A cells, which was further reduced by PARP1 silencing (Fig. 4C). Increased DNMT1 expression by PARP1 knockout may contribute to inhibition miR-126 expression via a methylation-dependent mechanism; miR-126 was restored in association with *EGFL7* when both DNMT1 and PARP1 were inhibited (Fig. 4E). Notably, PARP1 affected miR-222 expression, which was reduced in both Met-5A and H28 cells upon PARP1 silencing (Fig. 4D). A positive correlation was found between miR-222 and PARP1 levels ($r = 0.723$, $p = 0.032$).

Epigenetic regulation of miR-126 expression was then evaluated in malignant tissue of MM and adjacent non-malignant (NM) tissue, by way of evaluation of miR-126, *EGFL7* expression and the methylation status of the *EGFL7* S2 promoter region. Downregulation of both miR-126 and EGFL7 found in MM tissues were unrelated to any methylation changes within the *EGFL7* S2 promoter (Fig. 5A). On the other hand, high level of PARP1 and DNMT1 expression was observed in malignant compared to non-malignant tissue (Fig. 5B). Linear regression analysis revealed that expression of *EGFL7* and miR-126 correlated positively with each other and negatively with PARP1 and DNMT1 levels (Fig. 5C).

4. Discussion

In the present study, an *in vitro* model of asbestos-induced cell transformation was performed to evaluate the mechanism by which asbestos can regulate miR-222 and miR-126 expression. Exposure to asbestos induced time-dependent miR-222 and miR-126 upregulation, which was potentiated by the stroma environment (*cf* Fig. 1), supporting the role of cancer stroma in regulation of miR-126 as previously reported (Huang and Chu, 2014).

Both inflammation and asbestos exposure induced miR-222 expression, which was reversed by inhibiting the EGFR pathway, thus pointing to its involvement (*cf* Fig. 2). Regulation of miR-222 via EGFR activation was previously observed (Teixeira et al., 2012; Garofalo et al., 2011). Transactivation of EGFR stimulates downstream signaling pathways involved in regulating a wide variety of cellular functions, including cell proliferation, migration, adhesion, and differentiation. In this context, the miR-221/miR-222 cluster has been reported to be under the control of the Ras-MAPK pathway and to support tumor-associated neo-angiogenesis and invasion in neoplastic pathologies (Li et al., 2018; Abak et al., 2018). The protein Slug, by binding to the miR-221/miR-222 promoter, appears to be responsible for high expression of the miR-221/miR-222 cluster in breast cancer cells (Lambertini et al., 2012; Pan et al., 2016), EGFR being receptor orchestrating the Src/ERK/Slug pathway (Joannes et al., 2014). Increased expression of miR-222 was observed in cells exposed to air pollutants and to metal-rich particles (Vriens et al., 2016). Vascular expression of miR-222 was found to be upregulated in the initial atherogenic stages by means of inhibiting angiogenic recruitment of endothelial cells and via enhanced endothelial dysfunction (Chistiakov et al., 2015).

In this context, miR-126, a regulator of the MAPK signaling pathway, ameliorates endothelial dysfunction via targeting the Sprouty-related EVH1 domain-containing protein 1 (SPRED1) (Lei et al., 2018). Further, miR-126 has been shown to promote angiogenesis by

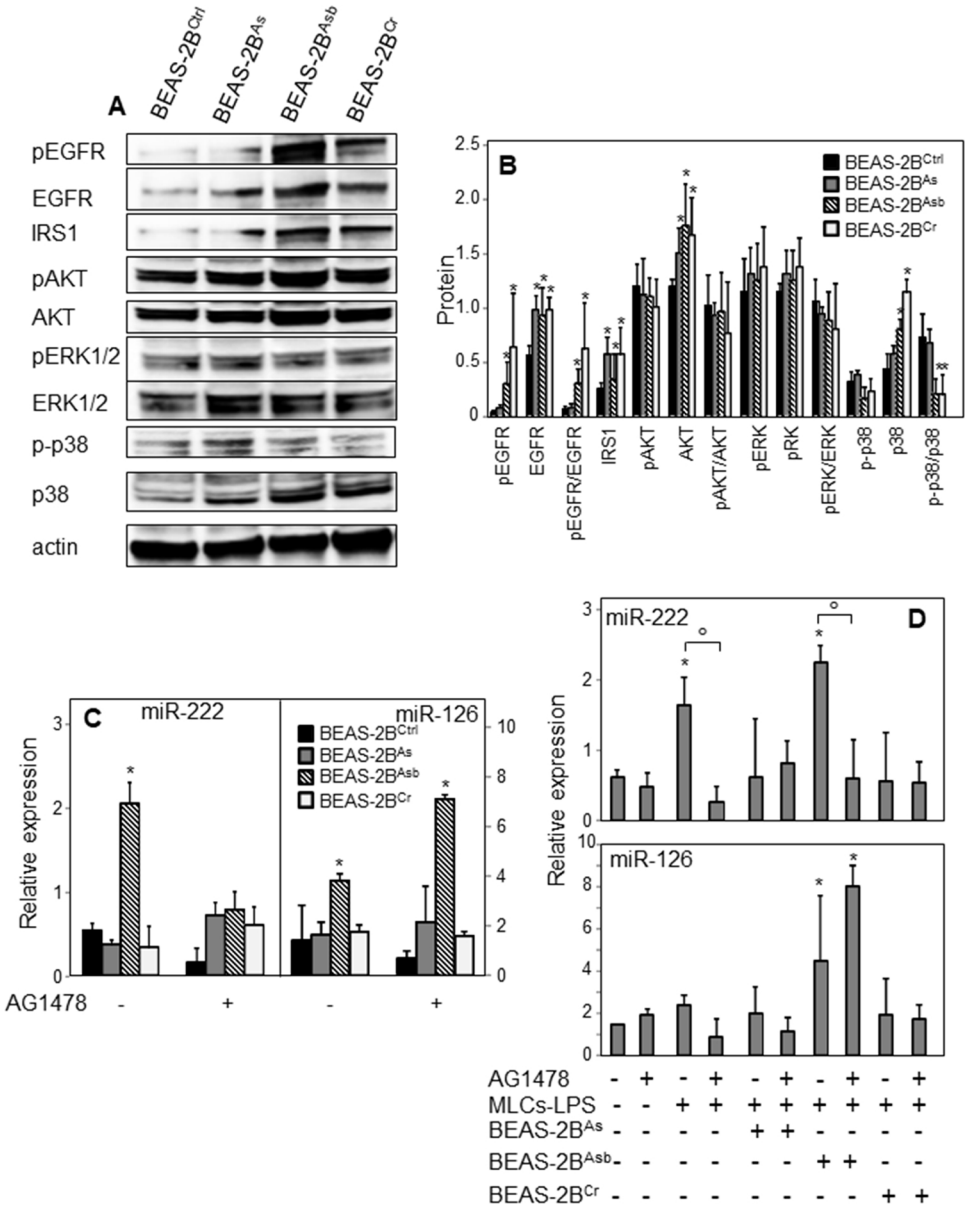

Fig. 2. Involvement of the EGFR pathway and inflammation on the miR-222 and miR-126 expression. A) Control, arsenic-, asbestos-, and chrome-transformed cells (BEAS-2B^{Ctrl}, BEAS-2B^{As}, BEAS-2B^{Asb} and BEAS-2B^{Cr} cells, respectively) were evaluated for the expression of the pEGFR, EGFR, IRS1, pAKT, AKT, pERK1/2, ERK1/2, p-p38, and p38 proteins by western blotting. B) The level of individual proteins shown in panel A was evaluated by densitometry related to actin. C) Expression of miR-222 and miR-126 evaluated in BEAS-2B^{Ctrl}, BEAS-2B^{As}, BEAS-2B^{Asb}, and BEAS-2B^{Cr} cells with and without an EGFR inhibitor AG1478. D) Expression of miR-222 and miR-126 evaluated in transformed BEAS-2B cells with and without an EGFR inhibitor AG1478, in the presence of cytokines induced by macrophage-like cells (MLCs) activated by liposaccharide (LPS). The data shown are mean values ± SD of three independent experiments. The symbol "*" indicates significant differences compared to BEAS-2B^{Ctrl}, and the symbol "°" indicates significant differences with and without AG1478, with $p < 0.05$.

repressing inhibitors of VEGF signaling, including SPRED1 and PIK3R2 (Fish et al., 2008), or to suppress tumor growth and tumor angiogenesis by directly targeting VEGF-A signaling (Chen et al., 2014).

We show here that upregulation of miR-126 expression was induced by exposure to asbestos in epithelial BEAS-2B cells, which was independent of EGFR activation. Although miR-126 upregulation was reported to be associated with oxidative stress, the mechanism miR-126 upregulation is not clear (Matsuzaki and Ochiya, 2018). In this context, aberrant promoter methylation is one of the mechanisms that regulate gene expression (Zhang et al., 2013; Cui et al., 2016; Andersen et al., 2015; Saito et al., 2009). DNA methyltransferases (DNMT1, DNMT3A and DNMT3B) in combination with the ten-eleven translocation (TET) family of proteins that catalyze demethylation, have been reported to regulate stress-induced miR-126 expression (Wang et al., 2018). Our results document that asbestos-induced miR-126 upregulation is not related to the methylation status of its host gene EGFL7 promoter, suggesting that other factors than DNA methylation itself at the CpG island promoter control miR-126 expression (*cf* Fig. 3). Since our results show that the EGFL7 promoter is not regulated by DNA methylation, we investigated possible structural changes of chromatin. Both DNMT1 and PARP1, which are known to modulate chromatin structure, were affected by asbestos exposure. Asbestos-induced DNMT1 expression paralleled reduced PARP1 levels (*cf* Fig. 3). The demethylating agent (5-aza-2′-dC) that reverts the locally hypermethylated phenotype, inhibited miR-126 expression in asbestos-transformed cells and their non-malignant counterparts, while inducing miR-126 expression in MM cells. As previously reported, the methylation status of a promoter does not always correlate with gene expression (Weber et al., 2007). A promoter with low level of CpGs or without CpGs in the 5′-UTRs may be regulated via DNA methylation. Similarly, hypermethylated CpG-containing promoters may be transcriptionally active. Methylation may play a permissive role by establishing chromatin structure changes, thus allowing transcriptional factors or histone modifications to regulate gene transcription (Tomasetti et al., 2019).

Inhibition of PARP1 activity as well as PARP1 silencing reduced miR-126 level in non-malignant epithelial and mesothelial cells, which was reversed when both PARP1 and DNMT1 were inhibited (*cf* Figs. 3 and 4). Conversely, knocking down PARP1 and DNMT1 reduced the expression of miR-126 and miR-222 in malignant mesothelioma cells. These processes support the notion of a role of DNMT1 and PARP1 interaction in the regulation of gene expression (Ciccarone et al., 2012; Sharma et al., 2016). PARP1 differentially interacts with the promoter

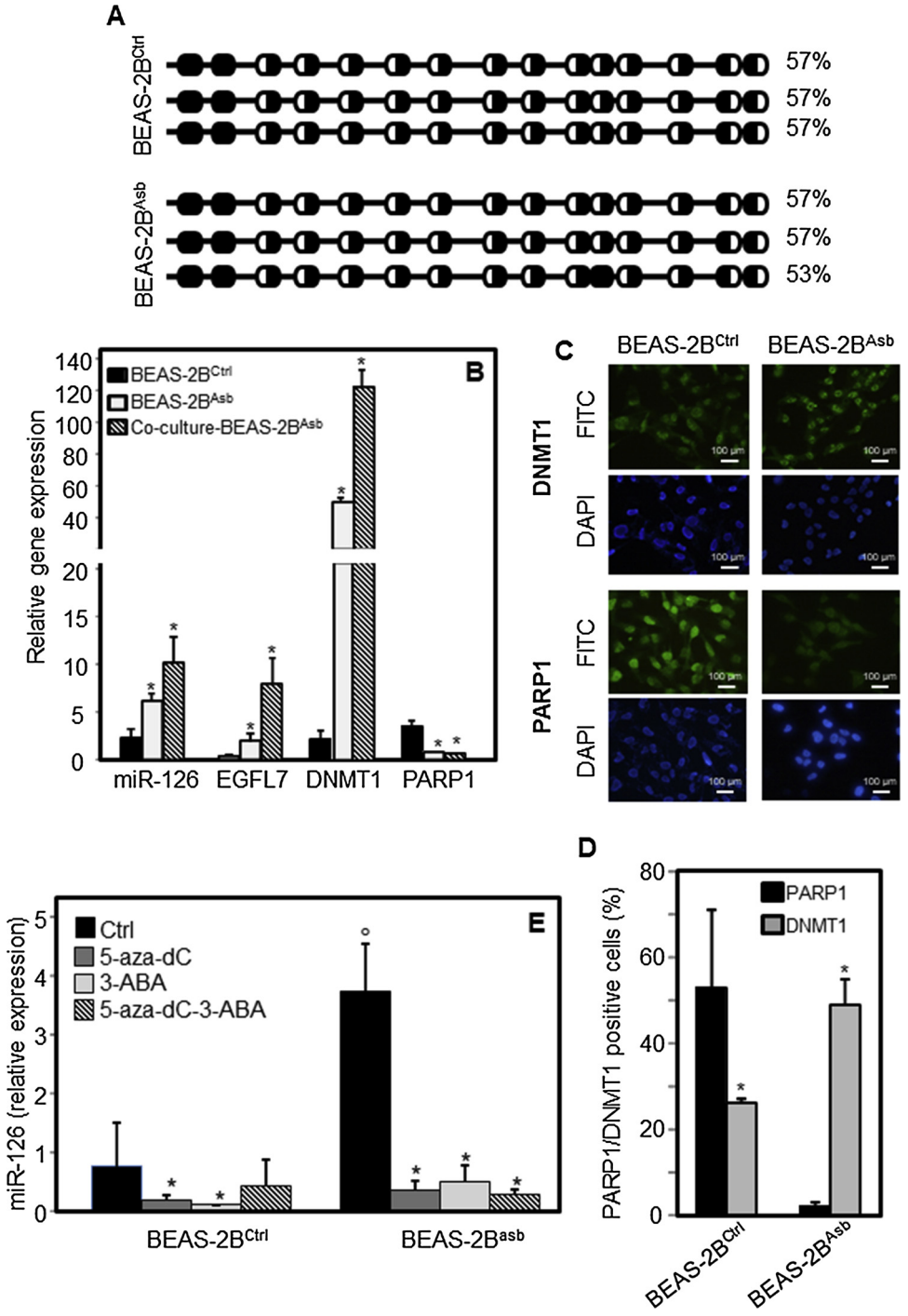

Fig. 3. Epigenetic regulation of miR-126 via changes in the methylation status and protein-related chromatin structure. A) Sequencing analysis of the CpG-island in T2 promoter of *EGFL7* that contains miR-126. Sequencing was performed using bisulfite-converted genomic DNA and the analyzed sequence was: AAC CCT TTA CTA ACT TTC AAA CCC. Methylation-susceptible CpG dinucleotides are shown including the percentage of relative C/T content. B) Expression of miR-126, *EGFL7*, DNMT1 and PARP1 in BEAS-2B^{Ctrl} and BEAS-2B^{Asb} cells in monoculture or in co-culture with fibroblasts (IMR-90) and endothelial cells (HUVEC). C) Immunocytochemistry of PARP1 and DNMT1 in BEAS-2B^{Ctrl} and BEAS-2B^{Asb}. D) The percentage of PARP1- and DNMT1-positive cells is presented. E) Expression of miR-126 in epithelial BEAS-2B cells and their asbestos-transformed counterpart (BEAS-2B^{Asb}) treated with 5-aza-2'-deoxycytidine (5-aza-dC, 5 µM, 96 h), with 3-aminobenzamide (3-ABA, 0.5 mM, 24 h), or with both 5-aza-dC and 3-ABA. The data shown are mean values ± S.D. derived from three independent experiments. The symbol "*" indicates significant differences compared with control, and the symbol "°" indicates significant differences between BEAS-2B^{Ctrl} and BEAS-2B^{Asb} cells, with $p < 0.05$.

region; it has been found that PARP1 silencing induced thrombomodulin promoter methylation in non-malignant mesothelial cells and demethylation in MM cells (Nocchi et al., 2011). Besides the role of the DNMT1 inhibitor in reversing gene expression changes associated with DNA methylation abnormalities in cancer, it has been reported that DNMT1 inhibition retains PARP1 within the chromatin fraction (Muvarak et al., 2016). In particular, PARP1 associates with promoters of actively transcribed genes and exerts both positive and negative effects on gene transcription (Ciccarone et al., 2017). In fact, PARP1 may affect a number of steps in gene expression via a series of physical and functional interactions with chromatin (Kraus and Hottiger, 2013).

Interestingly, miR-126 and EGFL7 were concomitantly expressed both in MM cells and tissues, such that tumors with higher EGFL7 mRNA expression showed comparably higher miR-126 levels. In addition, DNMT1 negatively correlated with both miR-126 and its host gene EGFL7 in MM tissues. These findings indicate that expression of DNMT1 is responsible for methylation of the EGFL7 promoter region, with ensuing downregulation of miR-126. However, we show that the methylation status of EGFL7 promoter cannot fully explain the modulation of miR-126 expression in the studied tissue and cells (*cf* Fig. 5). Rather than methylation itself, PARP1 orchestrates expression of miR-126 by its upregulation in asbestos-exposed cells, while downregulating miR-126 in MM cells.

As it has been proposed that PARP1 plays a role in the control of epigenetic processes, our results indicate a redundancy in the effect of PARPs on epigenetic regulation of the chromatin structure. We propose

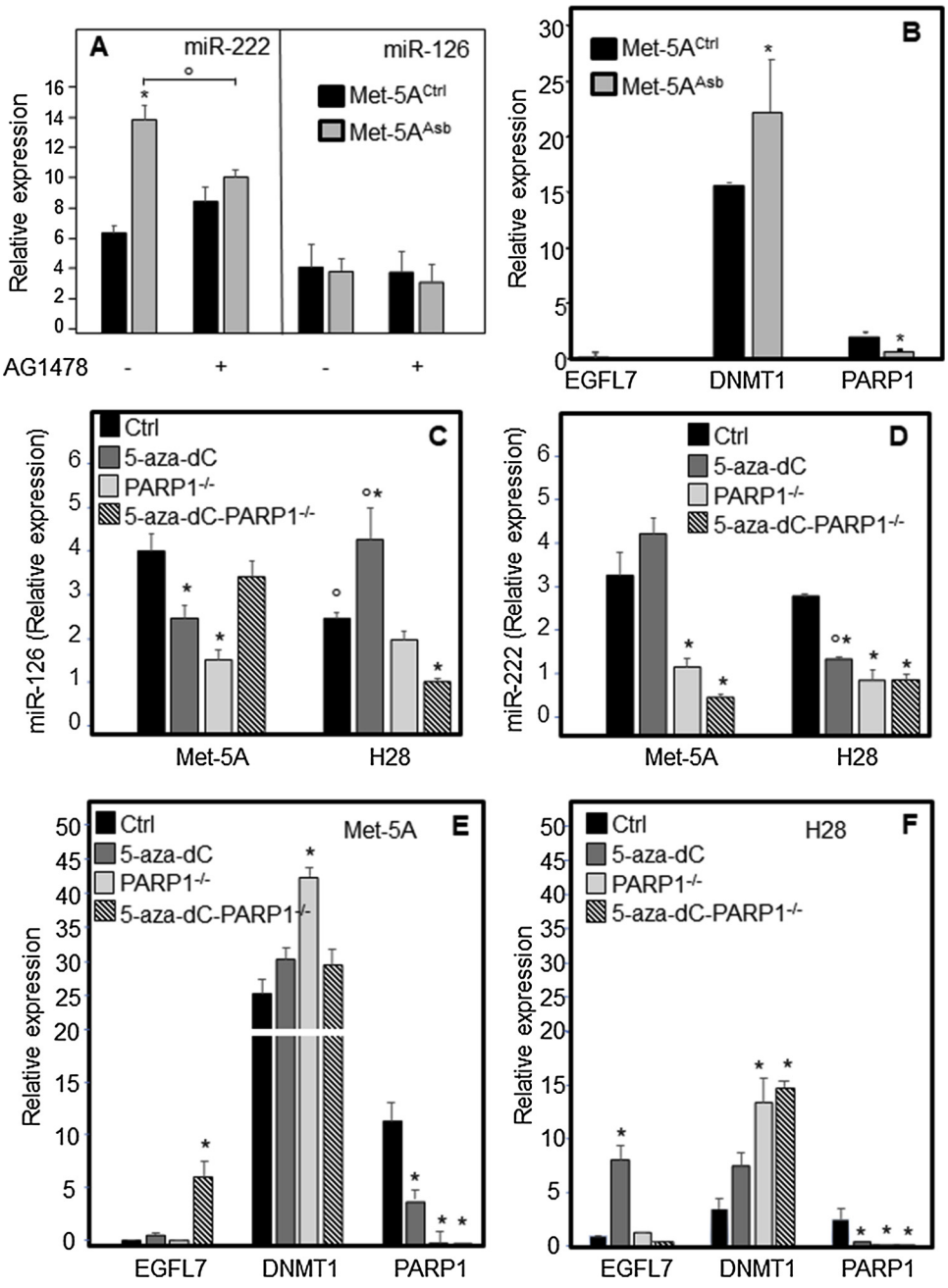

Fig. 4. Effect of asbestos exposure on miR-126 and miR-222 expression in mesothelial cells, and the role of DNMT1 and PARP1 in their expression in mesothelial cells and MM cells. A) Expression of miR-222 and miR-126 evaluated in non-malignant mesothelial (Met-5A^{Ctrl}) and asbestos-exposed Met-5A (Met-5A^{asb}) cells with and without the EGFR inhibitor AG1478. B) Expression of EGFL7, DNMT1 and PARP1 in asbestos-exposed and non-exposed mesothelial Met-5A cells (Met-5A^{Asb} and Met-5A^{Ctrl}). Expression of miR-126 (C) miR-222 (D) and *EGFL7*, DNMT1, PARP1 in non-malignant mesothelial Met-5A cells (E) and MM H28 cells (F) transfected with empty pRS plasmid (Ctrl) or with PARP1 shRNA pRS plasmid (PARP1$^{-/-}$) with and without 5-aza-2′-deoxycytidine (5-aza-dC) treatment. The data shown are mean values ± S.D. derived from three independent experiments. The symbol "*" indicates significant differences compared to the control, the symbol "°" indicates significant differences between Met-5A and H28 cells, with $p < 0.05$.

two mechanisms of asbestos-induced miRNA regulation. One of them implies activation of EGFR in response to asbestos exposure, while the other points to the involvement of epigenetic regulation, where PARP1 orchestrates miRNA expression. Both mechanisms, not being mutually exclusive, likely play an important role in asbestos-induced carcinogenesis and tumor growth.

Author contributions

S. G., and M. T. designed the experiments. S. G., F. M., and F. A. performed most experimental work. M. B., M. A., M. V., and A. S. performed patient enrolment and clinical evaluation. S. G., M. T., and L. S. performed data analysis and interpretation. J. N., and M. T. Written, review and revision of the manuscript. L. S., and A. T. performed study supervision.

Declaration of Competing Interest

The authors have no conflict of interest to declare.

Acknowledgments

This work was supported by grants 1/2011/5/n.1 from INAIL (National Institute for Insurance against Workplace Accidents and Occupational Disease), 1124/SPS/2016 from Region Friuli Venezia Giulia (Italy), and by the Czech Health Research Council grant (16-31704A) to Jiri Neuzil.

Appendix A. Supplementary data

Supplementary material related to this article can be found, in the online version, at doi:https://doi.org/10.1016/j.biocel.2020.105700.

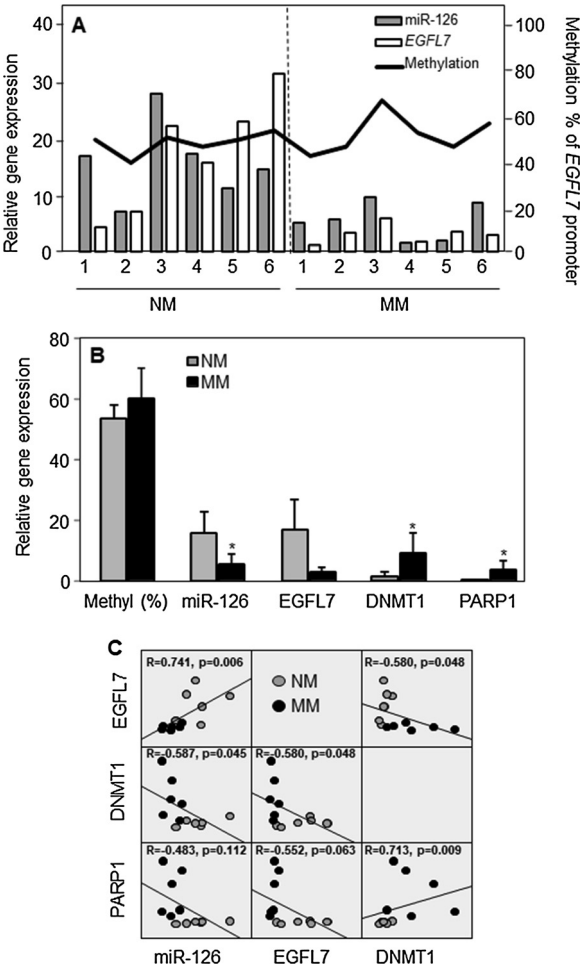

Fig. 5. Epigenetic regulation of miR-126 via changes in the methylation status of its host gene EGFL7 promoter, and expression of DNMT1 and PARP1 in biopsies. A) Methylation level of the EGFL7 promoter, miR-126 and *EGFL7* expression in six cases of patient-matched non-malignant (NM) and malignant mesothelioma (MM). B) Methylation status of EGFL7 promoter and levels of miR-126, *EGFL7*, DNMT1 and PARP1 in NM and MM biopsies. C) Correlation between miR-126, *EGFL7*, DNMT1 and PARP1. Correlation coefficient (R) was determined using the Spearman test. The symbol "*" indicates significant differences between NM and MM, wth $p < 0.05$.

References

Abak, A., Amini, S., Sakhinia, E., Abhari, A., 2018. MicroRNA-221: biogenesis, function and signatures in human cancers. Euro. Rev. Med. Pharmacol. Sci. 22, 3094–3117. https://doi.org/10.26355/eurrev_201805_15069.

Andersen, M., Trapani, D., Ravn, J., Sørensen, J.B., Andersen, C.B., Grauslund, M., Santoni-Rugiu, E., 2015. Methylation-associated silencing of microRNA-126 and its host gene EGFL7 in malignant pleural mesothelioma. Anticancer Res. 35, 6223–6229.

Carbonari, D., Campopiano, A., Ramires, D., Strafella, E., Staffolani, S., Tomasetti, M., Curini, R., Valentino, M., Santarelli, L., Amati, M., 2011. Angiogenic effect induced by mineral fibres. Toxicology 288, 34–42. https://doi.org/10.1016/j.tox.2011.06.016.

Chen, H., Li, L., Wang, S., Lei, Y., Ge, Q., Lv, N., Zhou, X., Chen, C., 2014. Reduced miR-126 expression facilitates angiogenesis of gastric cancer through its regulation on VEGF-A. Oncotarget 5, 11873–11885. https://doi.org/10.18632/oncotarget.2662. 2014.

Chistiakov, D.A., Sobenin, I.A., Orekhov, A.N., Bobryshev, Y.V., 2015. Human miR-221/222 in physiological and atherosclerotic vascular remodeling. Biomed. Res. Int., 354517. https://doi.org/10.1155/2015/354517. 2015.

Ciccarone, F., Klinger, F.G., Catizone, A., Calabrese, R., Zampieri, M., Bacalini, M.G., De Felici, M., Caiafa, P., 2012. Poly(ADP-ribosyl)ation acts in the DNA demethylation of mouse primordial germ cells also with DNA damage-independent roles. PLoS One 7, e46927. https://doi.org/10.1371/journal.pone.0046927.

Ciccarone, F., Zampieri, M., Caiafa, P., 2017. PARP1 orchestrates epigenetic events setting up chromatin domains. Semin. Cell Dev. Biol. 63, 123–134. https://doi.org/10.1016/j.semcdb.2016.11.010.

Cui, H., Mu, Y., Yu, L., Xi, Y.G., Matthiesen, R., Su, X., Sun, W., 2016. Methylation of the miR-126 gene associated with glioma progression. Fam. Cancer 15, 317–324. https://doi.org/10.1007/s10689-015-9846-4.

Deng, Q., Dai, X., Feng, W., Huang, S., Yuan, Y., Xiao, Y., Zhang, Z., Deng, N., Deng, H., Zhang, X., Kuang, D., Li, X., Zhang, W., Zhang, X., Guo, H., Wu, T., 2019. Co-exposure to metals and polycyclic aromatic hydrocarbons, microRNA expression, and early health damage in coke oven workers. Environ. Int. 122, 369–380. https://doi.org/10.1016/j.envint.2018.11.056.

Du, J., Zhang, L., 2015. Integrated analysis of DNA methylation and microRNA regulation of the lung adenocarcinoma transcriptome. Oncol. Rep. 34, 585–594. https://doi.org/10.3892/or.2015.4023.

Ebrahimi, F., Gopalan, V., Smith, R.A., Lam, A.K., 2014. miR-126 in human cancers: clinical roles and current perspectives. Exp. Mol. Pathol. 96, 98–107. https://doi.org/10.1016/j.yexmp.2013.12.004.

Ferrante, M., Conti, G.O., 2017. Environment and neurodegenerative diseases: an update on miRNA role. Microrna 6, 157–165. https://doi.org/10.2174/2211536606666170811151503.

Fish, J.E., Santoro, M.P.M., Morton, S.U., Yu, S., Yeh, R.F., Wythe, J.D., Ivey, K.N., Bruneau, B.G., Stainier, D.Y., Srivastava, D., 2008. miR-126 regulates angiogenic signaling and vascular integrity. Dev. Cell 15, 272–284. https://doi.org/10.1016/j.devcel.2008.07.008.

Garofalo, M., Romano, G., Di Leva, G., Nuovo, G., Jeon, Y.J., Ngankeu, A., Sun, J., Lovat, F., Alder, H., Condorelli, G., Engelman, J.A., Ono, M., Rho, J.K., Cascione, L., Volinia, S., Nephew, K.P., Croce, C.M., 2011. EGFR and MET receptor tyrosine kinase-altered microRNA expression induces tumorigenesis and gefitinib resistance in lung cancers. Nat. Med. 18, 74–82. https://doi.org/10.1038/nm.2577.

Huang, T.H., Chu, T.Y., 2014. Repression of miR-126 and upregulation of adrenomedullin in the stromal endothelium by cancer-stromal cross talks confers angiogenesis of cervical cancer. Oncogene 33, 3636–3647. https://doi.org/10.1038/onc.2013.335.

Joannes, A., Grelet, S., Duca, L., Gilles, C., Kileztky, C., Dalstein, V., Birembaut, P., Polette, M., Nawrocki-Raby, B., 2014. Fhit regulates EMT targets through an EGFR/Src/ERK/Slug signaling axis in human bronchial cells. Mol. Cancer Res. 12, 775–783. https://doi.org/10.1158/1541-7786.MCR-13-0386-T.

Kraus, W.L., Hottiger, M.O., 2013. PARP-1 and gene regulation: progress and puzzles. Mol. Asp. Med. 34, 1109–1123. https://doi.org/10.1016/j.mam.2013.01.005.

Lambertini, E., Lolli, A., Vezzali, F., Penolazzi, L., Gambari, R., Piva, R., 2012. Correlation between Slug transcription factor and miR-221 in MDA-MB-231 breast cancer cells. BMC Cancer 12, 445. https://doi.org/10.1186/1471-2407-12-445.

Lei, H., Li, H., Tian, L., Li, M., Xin, Z., Zhang, X., Guan, R., 2018. Icariside II ameliorates endothelial dysfunction by regulating the MAPK pathway via miR-126/SPRED1 in diabetic human cavernous endothelial cells. Drug Des. Devel. Ther. 12, 1743–1751. https://doi.org/10.2147/DDDT.S166734.

Li, Z., Tao, Y., Wang, X., Jiang, P., Li, J., Peng, M., Zhang, X., Chen, K., Liu, H., Zhen, P., Zhu, J., Liu, X., Liu, X., 2018. Tumor-secreted exosomal miR-222 promotes tumor progression via regulating P27 expression and re-localization in pancreatic cancer. Cell. Physiol. Biochem. 51, 610–629. https://doi.org/10.1159/000495281.

Liu, R., Gu, J., Jiang, P., Zheng, Y., Liu, X., Jiang, X., Huang, E., Xiong, S., Xu, F., Liu, G., Ge, D., Chu, Y., 2015. DNMT1-microRNA126 epigenetic circuit contributes to esophageal squamous cell carcinoma growth via ADAM9-EGFR-AKT signaling. Clin. Cancer Res. 21, 854–863. https://doi.org/10.1158/1078-0432.CCR-14-1740.

Liu, F., Zhang, H., Lu, S., Wu, Z., Zhou, L., Cheng, Z., Bai, Y., Zhao, J., Zhang, Q., Mao, H., 2018. Quantitative assessment of gene promoter methylation in non-small cell lung cancer using methylation-sensitive high-resolution melting. Oncol. Lett. 15, 7639–7648. https://doi.org/10.3892/ol.2018.8321.

Matsuzaki, J., Ochiya, T., 2018. Extracellular microRNAs and oxidative stress in liver injury: a systematic mini review. J. Clin. Biochem. Nutr. 63, 6–11. https://doi.org/10.3164/jcbn.17-123.

Matsuzaki, J., Suzuki, H., 2015. Role of MicroRNAs-221/222 in digestive systems. J. Clin. Med. 4, 1566–1577. https://doi.org/10.3390/jcm4081566.

Muvarak, N.E., Chowdhury, K., Xia, L., Robert, C., Choi, E.Y., Cai, Y., Bellani, M., Zou, Y., Singh, Z.N., Duong, V.H., Rutherford, T., Nagaria, P., Bentzen, S.M., Seidman, M.M., Baer, M.R., Lapidus, R.G., Baylin, S.B., Rassool, F.V., 2016. Enhancing the cytotoxic effects of PARP inhibitors with DNA demethylating agents - a potential therapy for cancer. Cancer Cell 30, 637–650. https://doi.org/10.1016/j.ccell.2016.09.002.

Nakamura, H., Jasper, M.J., Hull, M.L., Aplin, J.D., Robertson, S.A., 2012. Macrophages regulate expression of α1,2-fucosyltransferase genes in human endometrial epithelial cells. Mol. Hum. Reprod. 18, 204–215.

Nocchi, L., Tomasetti, M., Amati, M., Neuzil, J., Santarelli, L., Saccucci, F., 2011. Thrombomodulin is silenced in malignant mesothelioma by a poly(ADP-ribose) polymerase-1-mediated epigenetic mechanism. J. Biol. Chem. 286, 19478–19488. https://doi.org/10.1074/jbc.M110.217331.

Pache, J.C., Janssen, Y.M., Walsh, E.S., Quinlan, T.R., Zanella, C.L., Low, R.B., Taatjes, D.J., Mossman, B.T., 1998. Increased epidermal growth factor-receptor protein in a human mesothelial cell line in response to long asbestos fibers. Am. J. Pathol. 152, 333–340.

Pan, Y., Li, J., Zhang, Y., Wang, N., Liang, H., Liu, Y., Zhang, C.Y., Zen, K., Gu, H., 2016. Slug-upregulated miR-221 promotes breast cancer progression through suppressing E-cadherin expression. Sci. Rep. 6, 25798. https://doi.org/10.1038/srep25798.

Rao, X., Di Leva, G., Li, M., Fang, F., Devlin, C., Hartman-Frey, C., Burow, M.E., Ivan, M., Croce, C.M., Nephew, K.P., 2011. microRNA-221/222 confers breast cancer fulvestrant resistance by regulating multiple signaling pathways. Oncogene 30, 1082–1097. https://doi.org/10.1038/onc.2010.487.

Ruíz-Vera, T., Ochoa-Martínez, Á.C., Zarazúa, S., Carrizales-Yáñez, L., Pérez-Maldonado, I.N., 2019. Circulating miRNA-126, -145 and -155 levels in Mexican women exposed to inorganic arsenic via drinking water. Environ. Toxicol. Pharmacol. 67, 79–86. https://doi.org/10.1016/j.etap.2019.02.004.

Saito, Y., Friedman, J.M., Chihara, Y., Egger, G., Chuang, J.C., Liang, G., 2009. Epigenetic

therapy upregulates the tumor suppressor microRNA-126 and its host gene EGFL7 in human cancer cells. Biochem. Biophys. Res. Commun. 379, 726–731. https://doi.org/10.1016/j.bbrc.2008.12.098.

Santarelli, L., Gaetani, S., Monaco, F., Bracci, M., Valentino, M., Amati, M., Rubini, C., Sabbatini, A., Pasquini, E., Zanotta, N., Comar, M., Neuzil, J., Tomasetti, M., Bovenzi, M., 2019. Four-miRNA signature to identify asbestos-related lung malignancies. Cancer Epidemiol. Biomark. Prev. 28, 119–126. https://doi.org/10.1158/1055-9965.EPI-18-0453.

Sharma, V., Pandey, S.N., Khawaja, H., Brown, K.J., Hathout, Y., Chen, Y.W., 2016. PARP1 differentially interacts with promoter region of DUX4 gene in FSHD myoblasts. J. Genet. Syndr. Gene Ther. 7. https://doi.org/10.4172/2157-7412.1000303.

Song, J., Ouyang, Y., Che, J., Li, X., Zhao, Y., Yang, K., Zhao, X., Chen, Y., Fan, C., Yuan, W., 2017. Potential value of miR-221/222 as diagnostic, prognostic, and therapeutic biomarkers for diseases. Front. Immunol. 8, 56. https://doi.org/10.3389/fimmu.2017.00056.

Teixeira, A.L., Gomes, M., Medeiros, R., 2012. EGFR signaling pathway and related-miRNAs in age-related diseases: the example of miR-221 and miR-222. Front. Genet. 3, 286. https://doi.org/10.3389/fgene.2012.00286.

Tomasetti, M., Gaetani, S., Monaco, F., Neuzil, J., Santarelli, L., 2019. Epigenetic regulation of miRNA expression in malignant mesothelioma: miRNAs as biomarkers of early diagnosis and therapy. Front. Oncol. 9, 1293. https://doi.org/10.3389/fonc.2019.01293.

Vriens, A., Nawrot, T.S., Saenen, N.D., Provost, E.B., Kicinski, M., Lefebvre, W., Vanpoucke, C., Van Deun, J., De Wever, O., Vrijens, K., De Boever, P., Plusquin, M., 2016. Recent exposure to ultrafine particles in school children alters miR-222 expression in the extracellular fraction of saliva. Environ. Health 15, 1–9. https://doi.org/10.1186/s12940-016-0162-8. 2016.

Wang, X., Wang, S., Liu, W., Wang, T., Wang, J., Gao, X., Duan, R., Li, Y., Pu, L., Deng, B., Chen, Z., 2018. Epigenetic upregulation of miR-126 induced by heat stress contributes to apoptosis of rat cardiomyocytes by promoting Tomm40 transcription. J. Mol. Cell. Cardiol. 129, 39–48. https://doi.org/10.1016/j.yjmcc.2018.10.005.

Weber, M., Hellmann, I., Stadler, M.B., Ramos, L., Pääbo, S., Rebhan, M., Schübeler, D., 2007. Distribution, silencing potential and evolutionary impact of promoter DNA methylation in the human genome. Nat. Genet. 39, 457–466. https://doi.org/10.1038/ng1990.

Wei, T., Ye, P., Peng, X., Wu, L.L., Yu, G.Y., 2016. Prognostic value of miR-222 in various cancers: a systematic review and meta-analysis. Clinic. Lab. 62, 1387–1395. https://doi.org/10.7754/Clin.Lab.2016.160102.

Zhang, Y., Yang, P., Sun, T., Li, D., Xu, X., Rui, Y., Li, C., Chong, M., Ibrahim, T., Mercatali, L., Amadori, D., Lu, X., Xie, D., Li, Q.J., Wang, X.F., 2013. miR-126 and miR-126* repress recruitment of mesenchymal stem cells and inflammatory monocytes to inhibit breast cancer metastasis. Nat. Cell Biol. 15, 284–294. https://doi.org/10.1038/ncb2690.